THE JOURNAL OF BIOLOGICAL CHEMISTRY VOL. 284, NO. 38, pp. 26085–26095, September 18, 2009

Syndecan-1 Is Required for Robust Growth, Vascularization, and Metastasis of Myeloma Tumors *in Vivo*[*]

Received for publication, May 7, 2009, and in revised form, June 18, 2009 Published, JBC Papers in Press, July 13, 2009, DOI 10.1074/jbc.M109.018473

Yekaterina B. Khotskaya[‡1], **Yuemeng Dai**[§¶], **Joseph P. Ritchie**[‡‖], **Veronica MacLeod**[§], **Yang Yang**[‡‖**], **Kurt Zinn**[‡ ‡‡§§], **and Ralph D. Sanderson**[‡‖**2]

From the Departments of [‡]*Pathology,* [‡‡]*Radiology, and* [§§]*Medicine, the* ***Comprehensive Cancer Center, and the* [‖]*Center for Metabolic Bone Disease, University of Alabama at Birmingham, Birmingham, Alabama 35294 and the Departments of* [§]*Pathology and* [¶]*Otolaryngology, University of Arkansas for Medical Sciences, Little Rock, Arkansas 72205*

Myeloma tumors are characterized by high expression of syndecan-1 (CD138), a heparan sulfate proteoglycan present on the myeloma cell surface and shed into the tumor microenvironment. High levels of shed syndecan-1 in the serum of patients are an indicator of poor prognosis, and numerous studies have implicated syndecan-1 in promoting the growth and progression of this cancer. In the present study we directly addressed the role of syndecan-1 in myeloma by stable knockdown of its expression using RNA interference. Knockdown cells that were negative for syndecan-1 expression became apoptotic and failed to grow *in vitro*. Knockdown cells expressing syndecan-1 at ~28% or ~14% of normal levels survived and grew well *in vitro* but formed fewer and much smaller subcutaneous tumors in mice compared with tumors formed by cells expressing normal levels of syndecan-1. When injected intravenously into mice (experimental metastasis model), knockdown cells formed very few metastases as compared with controls. This indicates that syndecan-1 may be required for the establishment of multi-focal metastasis, a hallmark of this cancer. One mechanism of syndecan-1 action occurs via stimulation of tumor angiogenesis because tumors formed by knockdown cells exhibited diminished levels of vascular endothelial growth factor and impaired development of blood vessels. Together, these data indicate that the effects of syndecan-1 on myeloma survival, growth, and dissemination are due, at least in part, to its positive regulation of tumor-host interactions that generate an environment capable of sustaining robust tumor growth.

Multiple myeloma is an aggressive and deadly hematologic malignancy of plasma cells that resides predominantly in the bone marrow (1). The term "multiple" refers to the multifocal appearance of myeloma throughout the skeleton, which identifies the intrinsic ability of myeloma cells to metastasize extensively. Despite significant progress made in the last 20 years, myeloma remains incurable, often requiring aggressive therapeutic approaches leading to a multitude of adverse effects. New biologically based therapies such as the proteasome inhibitor Velcade, bisphosphonates, and thalidomide have proven effective in some patients. Success of these therapies, at least in part, is due to their impact on the tumor microenvironment (2). Interactions between myeloma cells and the bone clearly drive the progression of this cancer and are also important in mediating drug resistance (3–6). Thus, understanding the myeloma microenvironment is key to devising new strategies for therapeutic intervention.

Heparan sulfate proteoglycans are known to regulate the initiation and progression of some cancers (7–9). Syndecan-1 is a cell surface heparan sulfate-bearing proteoglycan that plays an important role in regulating myeloma (5). Syndecan-1 is expressed by all myeloma tumors within the bone marrow and is present in relatively high levels on the surface of most myeloma tumor cells (10, 11). The extracellular domain of this proteoglycan can be cleaved from the cell surface by sheddases, and high levels of shed syndecan-1 correlate with poor prognosis in myeloma patients (12). Shed syndecan-1 remains biologically active and can participate in regulating many cellular behaviors, including myeloma growth (13, 14). Much of syndecan-1 function is mediated by its heparan sulfate chains that bind to, and regulate the activity of, many of the factors known to influence myeloma growth (*e.g.* IL-6,[3] IL-7, IL-8, VEGF, HGF, fibroblast growth factor 2, and fibroblast growth factor family ligands). Signaling events propagated by these growth factors, particularly those events occurring between tumor cell and bone marrow components, are critical to the growth and development of myeloma (15). In addition, syndecan-1 becomes lodged within fibrotic regions of bone marrow following treatment of patients (11). This residual syndecan-1 may retain growth factors that aid in forming niches that facilitate tumor relapse. Thus, both on the cell surface and within the extracellular matrix, syndecan-1 is strategically placed to act as an important moderator of cross-talk between tumor and host cells, thereby promoting the growth and maintenance of the

* This work was supported, in whole or in part, by National Institutes of Health Grant CA055819 (to R. D. S.). This work was also supported by Comprehensive Cancer Center Core Support Grant P30CA013148 (to R. D. S.), University of Alabama at Birmingham Multi-Purpose Arthritis and Musculoskeletal Center Grant P30AR48311 (Flow Cytometry Core), and Institutional Training Grant Predoctoral Grant T32-AR047512 (to J. P. R.).

[1] Submitted this work in partial fulfillment of the requirements for a Ph. D., University of Alabama at Birmingham.

[2] To whom correspondence should be addressed: Dept. of Pathology, University of Alabama at Birmingham, 814 SHEL, 1530 Third Ave. S., Birmingham, AL 35294. Tel.: 205-996-6226; Fax: 205-996-6119; E-mail: sanderson@uab.edu.

[3] The abbreviations used are: IL, interleukin; ELISA, enzyme-linked immunosorbent assay; FACS, fluorescence-activated cell sorting; GFP, green fluorescent protein; HGF, hepatocyte growth factor; PBS, phosphate-buffered saline; RT, reverse transcription; SCID, severe combined immunodeficient; shRNA, small hairpin RNA; VEGF, vascular endothelial growth factor; ERK, extracellular signal-regulated kinase.

tumor as an "organ" and contributing to development of refractory disease.

We previously demonstrated in a limited study that knockdown of syndecan-1 expression inhibited growth of subcutaneous myeloma tumors (16). This is confirmed in the present work using a second shRNA targeting sequence and a different myeloma cell line. More importantly, we now demonstrate that disruption of syndecan-1 expression impacts two of the hallmarks of myeloma: angiogenesis and metastasis. When tumors do form from cells having low syndecan-1 expression, angiogenesis is initiated, but vessels fail to develop extensively, suggesting that tumor growth is limited by inadequate blood supply. Moreover, myeloma cells having low syndecan-1 expression are greatly impaired in their ability to form metastatic lesions following intravenous injection of cells, indicating that syndecan-1 may play a key role in driving the highly metastatic phenotype observed in essentially all myeloma patients. These results provide novel insight into regulation of myeloma tumor growth by syndecan-1.

EXPERIMENTAL PROCEDURES

Cell Lines and shRNA Knockdown—CAG (established from a myeloma patient's bone marrow aspirate at the Arkansas Cancer Research Center (17)) and RPMI-8226 (American Type Culture Collection, Manassas, VA) human myeloma cell lines were maintained in RPMI 1640 medium (Invitrogen) supplemented with 10% fetal bovine serum, 1% antibiotic/antimycotic, and L-glutamine (Mediatech, Herndon, VA). The cells were infected with lentiviral vectors delivering sequences for either a control shRNA sequence or shRNA targeting human syndecan-1 as described previously (16). The plates were maintained at 37 °C in humidified atmosphere with 5% CO_2. The shRNA targeting sequences were as follows: control, 5′-CGCGTCCCCGTCTCCGAACGTGTCACGTTTCAAGAGAACGTGACACGTTCGGAGACTTTTTGGAAAT-3′; *syn1A*, 5′-CGCGTCCCCGGAGGAATTCTATGCCTGATTCAAGAGATCAGGCATAGAATTCCTCCTTTTTGGAAAT-3′; and *syn1C*, 5′-CGCGTCCCCGGTAAGTTAAGTAAGTTGATTCAAGAGATCAACTTACTTAACTTACCTTTTTGGAAAT-3′. To rescue the phenotype of syndecan-1 knockdown cells, syn1A-transduced CAG myeloma cells were stably transfected with the pcDNA3 vector encoding full-length murine syndecan-1 cDNA (18). Transfected cells were selected with Geneticin (G418; Invitrogen), and murine syndecan-1 expression was confirmed by flow cytometry.

Flow Cytometry and Fluorescence-activated Cell Sorting (FACS)—To prepare cells for flow cytometry or FACS, the cells were collected by centrifugation and washed twice in PBS. The cell pellets were then resuspended in primary antibody (anti-human syndecan-1 (Diaclone, Canton, MA), anti-human CD20 (NeoMarkers, Fremont, CA), anti-human CD45 (NeoMarkers), anti-human CD38 (BD Biosciences, Bedford, MA), or anti-mouse syndecan-1 (281.2 antibody (19)) or anti-human syndecan-2 or syndecan-4 (kind gift from Dr. Anne Woods, University of Alabama at Birmingham, Birmingham, AL)) diluted in PBS and incubated on ice for 1 h. The cells were then washed three times in PBS and incubated with secondary antibody conjugated to Alexa 647 (Invitrogen) on ice for 1 h. Following incubation, the cells were washed three times in PBS and resuspended in either complete medium (for sorting by FACS) or PBS (for flow cytometry). The gates were set on the live cell population by side scatter/forward scatter first, followed by gating on the green fluorescent protein (GFP)-positive cells to ensure that cell sorting or analysis was limited to cells infected with the lentiviral construct. For cell cycle analysis, the cells were washed in PBS, fixed in ethanol on ice, and stained with propidium iodide solution containing 0.05% Triton X-100 for 40 min at 37 °C. FACS and flow cytometry were performed using a Becton Dickinson FACS VantageSE with DiVa option for FACS, FACScan with a 488-nm blue laser, or FACSCalibur with 488-nm blue and 635-nm red diode lasers for flow cytometry.

Western Blotting—For cell signaling studies, an equal number of myeloma cells were serum-starved overnight, followed by stimulation with 50 ng of recombinant HGF (R & D Systems) for 30 min. Cell extracts from an equal number of cells were prepared as previously described (20), separated on 10% or 4–15% gradient SDS-PAGE (Bio-Rad), transferred onto Nytran$^+$ nitrocellulose membrane (Whatman/Schleicher & Schuell, Florham Park, NJ), and probed with anti-syndecan-1 (Diaclone), phospho-ERK (Cell Signaling, Danvers, MA), phospho-Akt (Cell Signaling), or β-actin (Sigma-Aldrich) primary antibody. Alternatively, snap-frozen tumor xenografts were homogenized in lysis buffer (1:4 w/v, 0.05 M Tris-HCl, pH 8.0, 150 mM NaCl, 1% Nonidet P-40, 0.5% deoxycholate, 0.1% SDS), separated on 10% SDS-PAGE (Bio-Rad), transferred onto Nytran$^+$ membrane, and probed for syndecan-1 (21) (antibody kindly provided by Alan Rapraeger, University of Wisconsin-Madison) or β-actin (Santa Cruz Biotechnology, Santa Cruz, CA). Protein bands were visualized by chemiluminescence (GE Healthcare, Pittsburg, PA). Syndecan-1, because of the molecular heterogeneity of its heparan sulfate chains, ran as a smear above 150 kDa, and the β-actin band was detected between the 37- and 50-kDa markers.

Reverse Transcription (RT)-PCR—Total RNA from myeloma cells was extracted using Qiagen RNeasy kit (Valencia, CA), and RT-PCR was performed using a Qiagen OneStep RT-PCR kit according to the manufacturer's protocol. The primers used to detect human syndecan-1 and glyceraldehyde-3-phosphate dehydrogenase were described previously (16). The PCR products were separated on 1.2% agarose gel by electrophoresis, and the bands were visualized by ethidium bromide staining. PCR product sizes were 396 bp for syndecan-1 and 452 bp for glyceraldehyde-3-phosphate dehydrogenase, respectively.

In Vitro Cell Proliferation Assay—An equal number of control and syndecan-1 knockdown cells were plated in complete growth media, and the plates were maintained at 37 °C in 5% CO_2 for 5 days. Cell aliquots were taken every 24 h and stained with Trypan Blue (Invitrogen) to identify live cells, which were then counted on a hemocytometer.

Cell Density Assay—An equal number of control and syndecan-1 knockdown cells were plated in serum-free medium, and the plates were maintained at 37 °C in 5% CO_2 for 48 h. Cell density was assessed using the CellTiter 96 nonradioactive assay (Promega, Madison, WI).

Methylcellulose Colony Formation Assay—The colony formation assay was modified from Ref. 22. Briefly, 1×10^3 myeloma cells were plated in triplicate in 1 ml of plating medium consisting of 1.2% methylcellulose (R & D Systems), 10% fetal bovine serum, 200 mM L-glutamine, and 1×10^{-4} mol/liter β-mercaptoethanol in Iscove's modified Dulbecco's medium (Invitrogen). The plates were maintained at 37 °C in 5% CO_2 for 10 days, at which point colonies consisting of >50 cells were counted manually.

Quantification of VEGF in Myeloma Conditioned Media—Equal numbers of control and syndecan-1 knockdown CAG myeloma cells were plated in complete growth medium. After 48 h, the cells were pelleted by centrifugation, and the media conditioned by the myeloma cells were collected. The levels of human VEGF were assessed using an ELISA kit (BioSource, Camarillo, CA).

Xenograft Tumors—Prior to injection into animals, all of the cell lines were tested and confirmed to be negative for Mycoplasma using a mycoplasma detection kit (MP Biomedicals, Solon, OH). For the subcutaneous tumor model, 1×10^6 CAG or 5×10^6 RPMI-8226 control or syndecan-1 knockdown cells were injected into the dorsal flanks of male 5–6-week-old severe combined immunodeficient (SCID) mice. Although this model does not examine myeloma growth in bone marrow, the primary site of human myeloma tumors, it has been widely used to study myeloma tumor growth and to validate myeloma therapeutics (23). In addition, we have found that results related to tumor growth using the subcutaneous model parallel those from the SCID-hu model of myeloma (14, 16). The animals were monitored for 5–10 weeks after injection of tumor cells and mouse sera collected at 2-week intervals. For the experimental metastasis model, 5×10^6 CAG cells expressing firefly luciferase were injected intravenously via the lateral tail vein into 3–4-week-old male SCID mice. The animals were imaged on an IVIS-100 system (Xenogen Corporation) 24 h after cell implantation and once weekly thereafter. The images were collected on mice under isoflurane anesthesia at 10–15 min after intraperitoneal injections of 2.5 mg of D-luciferin. The images were collected on mice always placed in the same ventral and dorsal positions for each imaging session. Imaging acquisition time ranged from 30 to 300 s depending on the time after cells were injected. The serum was collected weekly, and the animals were euthanized 5 weeks after tumor cell injection. Prior to euthanasia, the animals were injected with the D-luciferin, imaged, and then imaged again following removal of visceral organs to detect the presence of bone lesions with increased sensitivity. All of the animal experiments were reviewed and approved by the University of Alabama at Birmingham Institutional Animal Care and Use Committee prior to initiation.

Quantification of Human Immunoglobulin Light Chain—Human immunoglobulin κ (for CAG cells) or λ (for RPMI-8226 cells) light chain levels were measured in murine sera to assess whole animal tumor burden. Sera collected during animal studies were stored at −80 °C and analyzed by ELISA (Bethyl Laboratories, Montgomery, TX) in duplicate as described previously (14).

Quantification of Human Syndecan-1 in Xenograft Tumors—10 μg of total tumor protein was analyzed for levels of human syndecan-1 by Eli-pair ELISA kit (Diaclone). Amount of syndecan-1 was quantified as number of nanograms of syndecan-1 in each μg of tumor. The data shown are from a single animal study with five control and four syndecan-1 knockdown tumors.

Immunohistochemistry and Cytospin Analyses—Immunohistochemistry was performed on formalin-fixed, paraffin-embedded tissue sections. Briefly, the sections were deparaffinized and hydrated through a series of xylene and graded alcohol washes, followed by antigen retrieval in 10 mM sodium citrate buffer, pH 6.0. The endogenous peroxidase activity was quenched by incubating the sections in 3% H_2O_2 and blocking nonspecific antigen-binding sites with 5% bovine serum albumin in PBS. The sections were incubated overnight at 4 °C with primary antibodies against human syndecan-1 (Diaclone), human VEGF (NeoMarkers), mouse CD34 (Hycult Biotechnology, Canton, MA), or murine syndecan-1 (281.2 antibody (19)). Primary antibody was omitted for negative control. After the primary antibody, the sections were washed and incubated in appropriate biotin-conjugated secondary antibodies (Vector Laboratories, Burlingame, CA). Antibody complexes were visualized using diaminobenzidine from Vector Laboratories. For cytospin analyses, the cells were spun onto glass slides using a Cytospin 3 Cell Preparation System (Shandon Scientific, Astmoor, UK), dried at room temperature, and fixed in ice-cold methanol. Nonspecific binding sites were blocked by 5% bovine serum albumin in PBS. The slides were incubated overnight at 4 °C with the primary anti-human syndecan-1 (Diaclone), anti-cleaved caspases-3 (Cell Signaling, Boston, MA), or anti-mouse IgG1 control (Diaclone) antibodies for 1 h with biotin-conjugated secondary antibodies and visualized with diaminobenzidine. All of the slides were counterstained with Gill's formulation 2 hematoxylin. Immunohistochemistry and cytospin photographic images were taken using a Nikon microscope with a SPOT camera. Blood vessel length was measured using the National Institutes of Health ImageJ software.

Affymetrix Gene Array—Myeloma cells were plated in triplicate and grown in complete medium. Total RNA was extracted using Qiagen RNeasy kit, and samples were analyzed on Affymetrix GeneChip Gene ST arrays by the University of Alabama at Birmingham Comprehensive Cancer Center Gene Expression Core Facility.

Statistical Analysis—The data were analyzed using Student's t test for two samples assuming equal variances. The results with $p < 0.05$ were considered significant.

RESULTS

Myeloma Cells Undergo Apoptosis When Syndecan-1 Is Absent—To examine the effects of syndecan-1 in myeloma, we first attempted to completely knock out syndecan-1 expression in CAG, RPMI-8226, and U266 human myeloma cell lines via transfection with antisense RNA. In each of several attempts and employing three distinct antisense constructs, when cells without syndecan-1 expression were sorted and placed in culture, they died within 48 h.[4] Similarly, when syndecan-1 was knocked down in CAG cells using shRNA and the syndecan-1-

[4] V. MacLeod, Y. Yang, and R. Sanderson, unpublished observation.

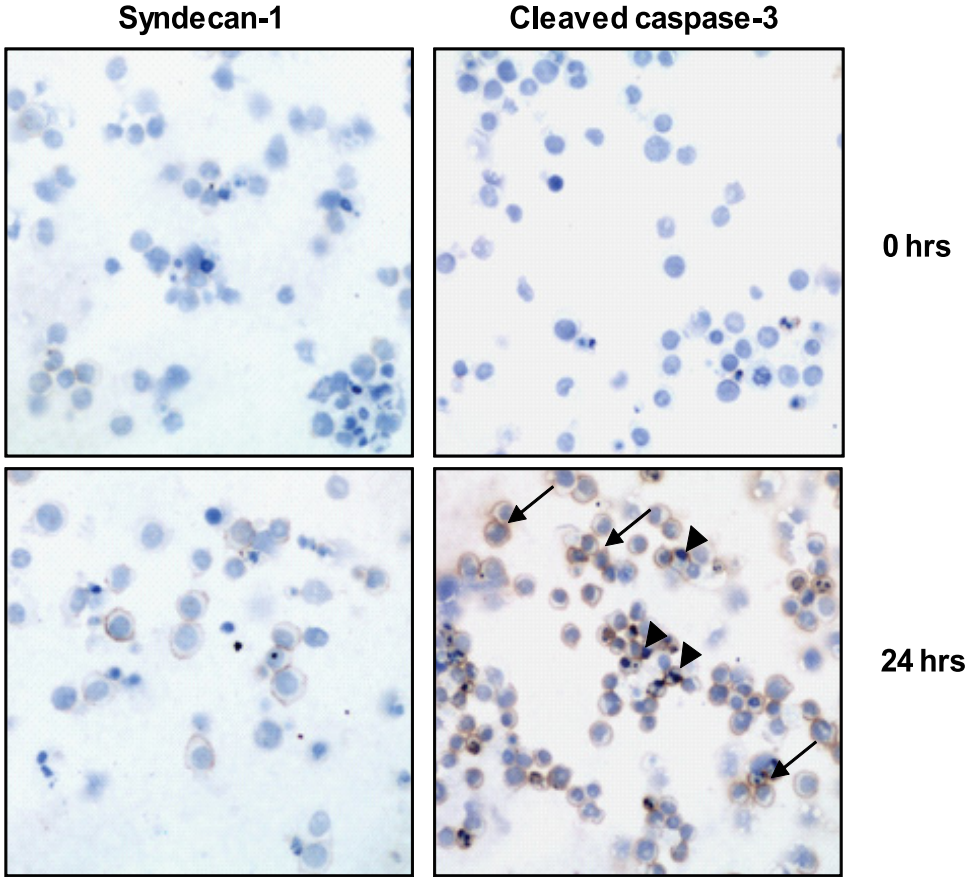

FIGURE 1. **Syndecan-1-negative myeloma cells undergo apoptosis *in vitro*.** CAG myeloma cells were transduced with a lentiviral vector delivering syn1A shRNA sequence. The cells were sorted by FACS to select the syndecan-1-negative population. Cytospin preparations immunostained for syndecan-1 immediately following cell sorting confirm that the cells are negative for syndecan-1 expression and for cleaved caspase-3. 24 h after cell sorting, a number of cells stain positively for cleaved caspase-3, indicating that they are undergoing apoptosis (brown reaction product, *arrows*; original magnification, ×200). The slides were counterstained with hematoxylin to identify nuclei. The *arrowheads* point to condensed nuclei indicative of apoptotic cell death.

negative cells were sorted and placed in cell culture, they became apoptotic within 24 h and failed to grow (Fig. 1). Thus, syndecan-1 expression at some base-line level is required for survival of these myeloma cell lines *in vitro*.

Myeloma Cells Expressing Syndecan-1 at Reduced Levels Grow Well in Vitro but Not in Vivo—We next examined the behavior of cells that expressed syndecan-1, but at levels reduced from that of wild-type CAG myeloma cells. Following transduction with lentiviral vectors coding for syndecan-1 shRNA, as determined by flow cytometry, syndecan-1 expression was knocked down to ~14% (syn1A shRNA) and ~28% (syn1C shRNA) of the normal levels present in cells transduced with control shRNA (Fig. 2*A*). To determine whether knockdown of syndecan-1 altered the phenotype of these cells, we assessed cell surface marker expression on the syn1A cells. Both the control and knockdown cells were positive for expression of CD38, a glycoprotein present on cells of myeloid and lymphoid lineages but absent from resting lymphocytes (Fig. 2*B*). In addition, the cells were negative for CD20, a marker expressed throughout the development of B lymphocytes with the exception of pro-B and plasma cells. Control and knockdown cells were also negative for CD45, a molecule that regulates antigen-mediated signaling and activation of lymphocytes but is absent from most clonogenic plasma cells. These findings demonstrate that the knockdown cells retain their mature plasma cell ($CD38^+/CD45^-$) phenotype and do not show signs of dedifferentiation. Examination of syndecan-2 and syndecan-4 expression revealed that these were not up-regulated upon knockdown of syndecan-1 (Fig. 2*B*). Previous studies have demonstrated that syndecan-3 is not expressed in CAG cells (24).

The *in vitro* growth properties of syn1A knockdowns were also similar to controls as assessed by cell counting, 3-(4,5-dimethylthiazol-2-yl)-2,5-diphenyltetrazolium bromide assay, colony forming assays and cell cycle analysis (Fig. 3, *A–C*). This similar growth pattern suggests that cell signaling pathways related to cell growth *in vitro* are not affected by diminished syndecan-1 expression. We tested this by treating cells with HGF, a major myeloma growth factor that requires syndecan-1 for its signaling via the Met receptor (25). The results show that levels of phosphorylated ERK are similar in control and knockdown cells (Fig. 3*D*). This suggests that even when syndecan-1 expression is reduced, there is sufficient syndecan-1 present to promote HGF signaling. Further indication of the similarity between the control and syn1A knockdown cells were results from Affymetrix gene arrays, which revealed they had almost identical patterns of gene expression. In addition to the anticipated difference in syndecan-1 expression, only four genes (SOHLH2, RCN2, LOC644714, and MAGEC2) had greater than a 2-fold change in expression between control and knockdown cells (and none of these changes were greater than 2.65-fold). Taken together, these data indicate that syn1A knockdowns, having ~14% of the normal level of syndecan-1 expression, retain their plasma cell phenotype and have growth properties *in vitro* that are similar to cells expressing wild-type levels of syndecan-1.

We next tested the ability of syndecan-1 knockdown cells to form tumors in mice. Previous limited studies with the syn1A cells indicate they have a reduced ability to grow when injected subcutaneously in mice as compared with control cells (16). When we compared control, syn1A, and syn1C cells *in vivo*, the extent of their growth correlated with the amount of syndecan-1 expressed (Fig. 4*A*). As syndecan-1 levels decreased, tumor burden decreased significantly, suggesting that the level of syndecan-1 expression regulates the extent of *in vivo* tumor growth.

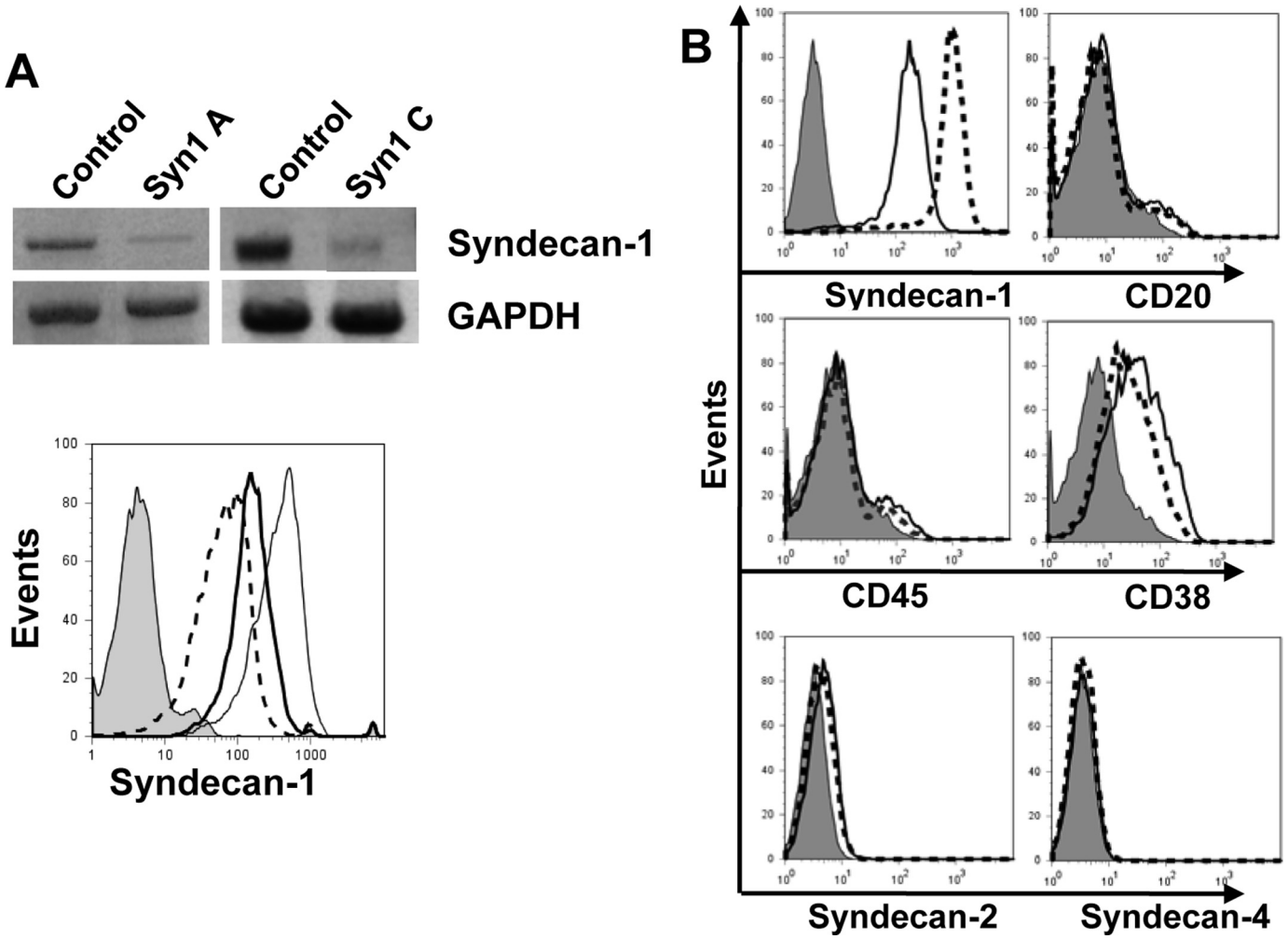

FIGURE 2. **shRNA reduces expression of syndecan-1 but does not alter the myeloma cell phenotype.** *A*, CAG myeloma cells were transduced with lentiviral vectors delivering control, syn1A, or syn1C shRNA sequences. Stable knockdown of syndecan-1 was confirmed by RT-PCR (*top panel*) and flow cytometry (*bottom panel*): IgG control antibody (*shaded*), control cells expressing wild-type levels of syndecan-1 (*thin solid line*), syn1A cells (*dashed line*), and syn1C cells (*thick solid line*). *B*, control cells (*dashed line*) and syn1A knockdown cells (*solid line*) were stained for markers of B cell lineage CD20, CD38, and CD45, or for syndecan-1, -2, or -4, or with control IgG antibody (*shaded peak*) and analyzed by flow cytometry. The gates were set on live, GFP+ cells. *GAPDH*, glyceraldehyde-3-phosphate dehydrogenase.

Immunohistology of sections of tumors formed by the syn1A cells revealed that, as expected, the knockdown cells remained positive for syndecan-1 following their injection into mice (Fig. 4*B*). Staining of the tissue for murine syndecan-1 revealed a pattern different from that of human syndecan-1, confirming the presence of human syndecan-1 produced by the tumor cells along with murine syndecan-1 within the stroma. Staining for GFP demonstrates that the cells forming the tumors were derived from cells transduced with the shRNA-containing lentivirus (Fig. 4*B*). Quantification of the levels of syndecan-1 by ELISA and Western blotting confirmed that the tumors formed by the syn1A cells had significantly less human syndecan-1 present as compared with controls (Fig. 4, *C* and *D*). The Western blot also reveals that the molecular size of the syndecan-1 proteoglycan in tumors formed by knockdown and control cells is similar. This indicates that knockdown of syndecan-1 did not substantially alter the amount of glycosylation present on the syndecan-1 core protein.

Inhibition of Tumor Growth in Vivo Is Not Cell Line-dependent—Similar to what was found with CAG cells, transduction with the syn1A shRNA construct significantly reduced levels of syndecan-1 expression in RPMI-8226 cells (Fig. 5*A*). As observed with the CAG cells, knockdown of syndecan-1 in RPMI-8226 cells had no effect on their *in vitro* growth rate. Upon subcutaneous injection of RPMI-8226 control and knockdown cells into SCID mice, only a single small (0.1 g) tumor developed in one mouse injected with the knockdown cells (Fig. 5*B*). In contrast, five of five animals injected with cells carrying the control shRNA sequence developed tumors. Because only one visible tumor arose from the knockdown cells, we quantified levels of human immunoglobulin λ light chain in the mouse sera to ensure that tumors had not formed extensive metastases (RPMI-8226 cells make and secrete high levels of this light chain). Fig. 4*C* shows that only very low levels of λ light chain were detected in the sera of animals injected with knockdown cells. Overall, data generated with the RPMI-8226 cells are similar to those obtained with the CAG cell line, further confirming that knockdown of syndecan-1 inhibits growth of myeloma cell lines *in vivo*.

Knockdown of Syndecan-1 Expression Inhibits Multifocal Disseminated Growth in a Model of Experimental Metastasis—To assess the behavior of syndecan-1 knockdown cells in an

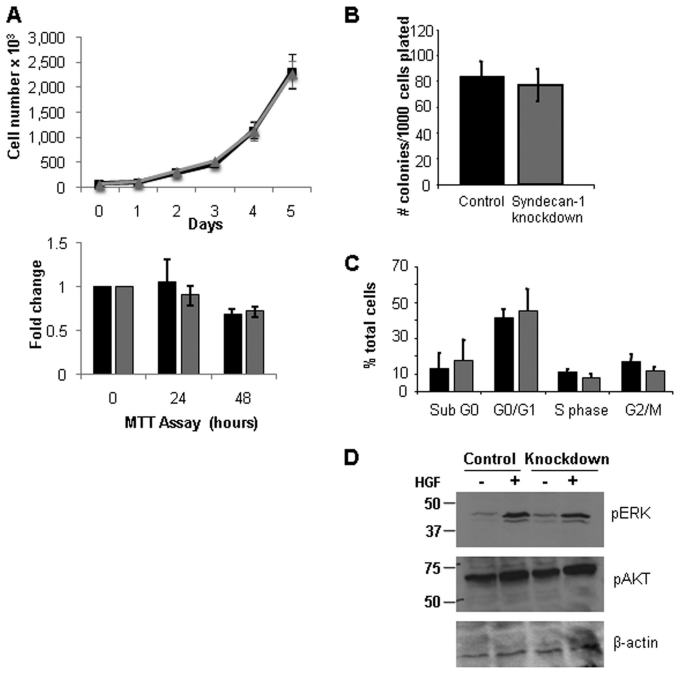

FIGURE 3. **Reduction in the level of syndecan-1 expression does not alter the *in vitro* growth characteristics of the CAG myeloma cells.** *A, upper panel*, equal number of control or syndecan-1 knockdown cells were plated in complete growth medium, and the cell numbers were assessed by direct counts. A single experiment representative of three independent assessments is shown. The data are the means ± S.D. *Lower panel*, equal numbers of control (*black bar*) and syndecan-1 knockdown (*gray bar*) cells were plated in serum-free medium, and cell density was determined by the 3-(4,5-dimethylthiazol-2-yl)-2,5-diphenyltetrazolium bromide (*MTT*) assay. The data are the means ± S.E. ($n = 3$). *B*, control and knockdown cells were plated in semi-solid methylcellulose media in triplicate. Following 10 days of growth, the number of colonies consisting of over 50 cells was manually counted. The data are the means ± S.E. ($n = 3$). *C*, 10^6 control (*black bars*) or knockdown (*gray bars*) cells were fixed in ethanol, stained with propidium iodide, and analyzed for DNA content on FACSCalibur. The data are the means ± S.E. ($n = 3$). *D*, equal number of CAG control or syndecan-1 knockdown cells were serum-starved overnight and then treated with recombinant HGF for 30 min. Cell lysates were analyzed for expression of phospho-ERK, phospho-Akt, and β-actin by immunoblotting.

animal model where myeloma is widely disseminated and thus mimics the human disease, control or knockdown CAG cells expressing luciferase were injected intravenously, and the animals were monitored for disease progression. Bioluminescence imaging revealed that the syndecan-1 knockdown cells were significantly less capable of forming tumors than were controls (Fig. 6*A*). A mean of 5.89 ± 0.6 lesions/animal were present in animals injected with control cells as compared with 1.0 ± 0.3 lesion/animal in animals injected with knockdown cells ($p = 0.0000005$, $n = 20$ animals/group). This was further confirmed by assessing levels of human immunoglobulin κ light chain in mouse sera. At the time of euthanasia, the mean human κ light chain levels were 527.6 ± 129.3 ng/ml in the control and 25.1 ± 18.6 ng/ml in the knockdown group, correlating well with bioluminescence images (Fig. 6*B*).

Because many of the animals injected with control cells had visceral tumors (predominantly in the liver), bioluminescent images were also collected after removal of visceral organs (Fig. 6*A*, *arrows* point to images of animals following removal of visceral organs). These images revealed that substantial amounts of tumor were present in the femora, spines, and ribs of the animals injected with control cells. In contrast, sensitive bioluminescence imaging did not detect tumors in bones of animals injected with knockdown cells even though a few animals had tumors growing in their visceral organs (2.6 ± 0.4 bone lesions/animal in controls; 0.2 ± 0.1 bone lesions/animal in knockdowns; $p = 0.00004$, $n = 10$ animals/group). Together these data reveal that cells expressing reduced levels of syndecan-1 form metastatic lesions poorly, even in the highly supportive bone marrow microenvironment.

To ensure that the difference in the *in vivo* growth of knockdown and control cells was not due to off target effects of the shRNA being utilized, the syn1A knockdown cells were transfected with a vector coding for the full-length murine syndecan-1 cDNA. Expression of the murine syndecan-1 was verified (Fig. 6*C*), and cells were injected into the tail veins of SCID mice. The results show that expression of the murine syndecan-1 restored the ability of the knockdown cells to grow *in vivo* to levels similar to those of control cells expressing wild-type levels of human syndecan-1 (Fig. 6*D*).

Tumors Formed by Syndecan-1 Knockdown Cells Exhibit Poorly Developed Vasculature and Decreased Levels of VEGF—Because there are no differences in phenotype or growth between knockdown and control cells *in vitro* (Figs. 2 and 3) but there major differences between their growth *in vivo*, this suggests that the growth promoting effects of syndecan-1 *in vivo* may be related to its effect on the tumor microenvironment. Thus, because vascularization of tumors is required for their extended growth and because heparan sulfate is known to promote angiogenesis via its interactions with pro-angiogenic growth factors, we assessed the microvessel density in tumors formed by control and knockdown cells (Fig. 7*A*). Although we found no difference in microvessel density, a considerable difference was noted in vessel quality. In tumors formed by the control cells, microvessels were long and branched, whereas in tumors formed by knockdown cells vessels were small and unbranched. Measurement of microvessel length revealed that on average, vessels in tumors formed by syndecan-1 knockdown cells were 50% shorter than those in the control group. This finding is consistent with recent studies in our lab demonstrating that syndecan-1 produced by CAG myeloma cells can enhance the motility and invasion of endothelial cells.[5]

Because VEGF is an important regulator of tumor vascularization, responsible for both the initiation of neoangiogenesis and microvessel maturation (26), we assessed its expression in tumors formed from control and knockdown cells. A striking difference in VEGF levels was observed, with the tumors formed by syndecan-1 knockdown cells having much less detectable VEGF (Fig. 7*B*). Quantification of VEGF levels *in vitro* revealed that the knockdown cells secreted significantly less VEGF than control cells (Fig. 7*C*). VEGF message levels *in vitro* were similar in control and knockdown cells, thus suggesting that regulation of VEGF is post-transcriptional.[6] Taken together, these data indicate that decreased levels of VEGF may lead to the impaired vascularization of tumors and the resulting poor tumor growth.

[5] A. Purushothaman, T. Uyama, and R. Sanderson, unpublished observation.
[6] Y. Khotskaya and R. Sanderson, unpublished observation.

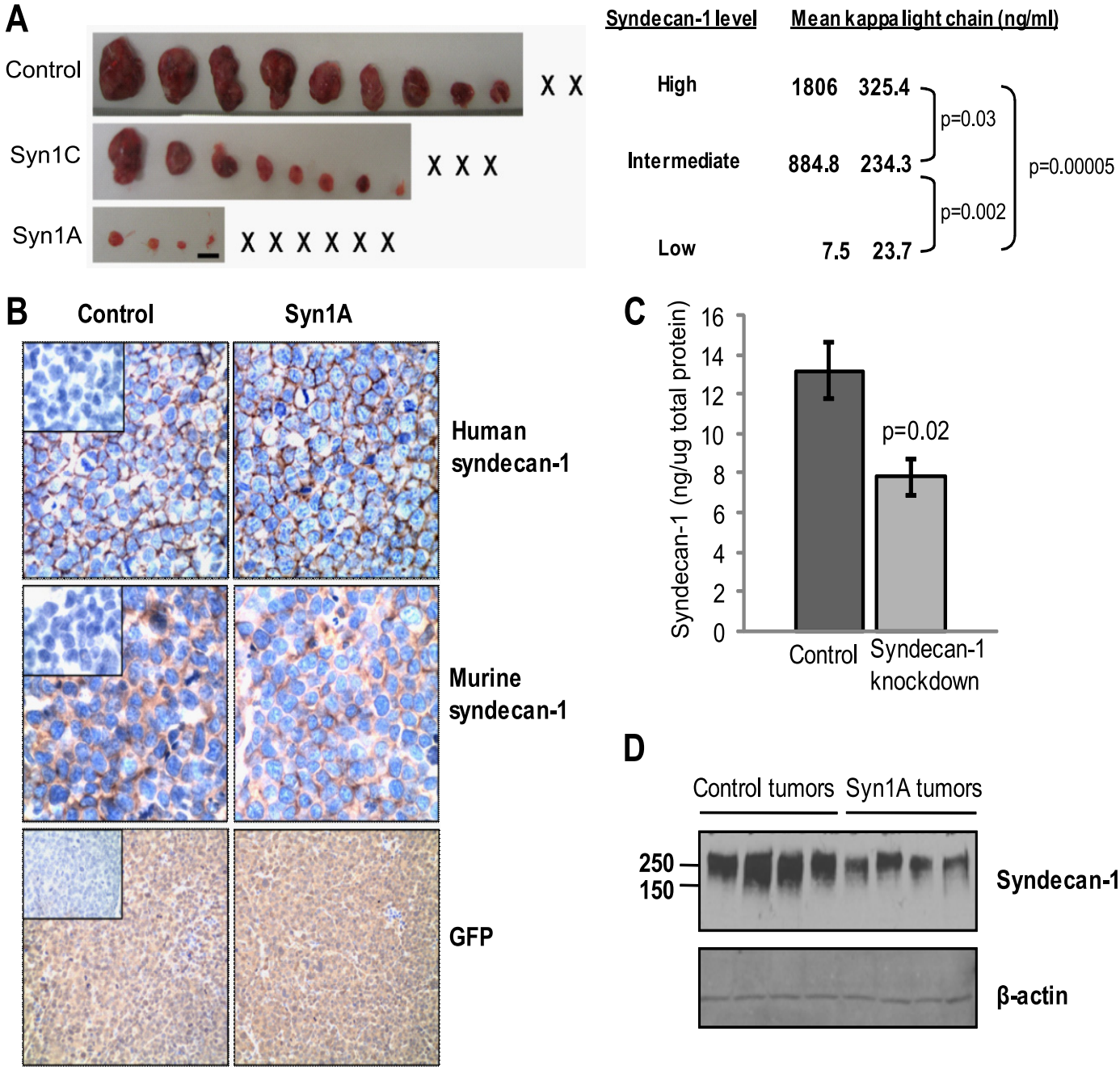

FIGURE 4. **Knockdown of syndecan-1 expression diminishes subcutaneous growth of myeloma cells.** *A*, 5 weeks after subcutaneous injection of control and syndecan-1 knockdown CAG cells into flanks of male SCID mice, the tumors were removed at necropsy and photographed (× represents animals with no detectable tumor; *bar*, 1 cm). The levels of human κ light chain in the serum were measured by ELISA and reflect the tumor burden in the mice 4 weeks after injection of tumor cells. *B*, immunohistochemical analysis of tumors for human and murine syndecan-1 (original magnification, ×400) and GFP expression (original magnification, ×200) are shown. *Insets*, negative control. *C*, tissue extracts prepared from tumors formed by the control ($n = 5$) and syn1A ($n = 4$) cells were analyzed by ELISA for levels of human syndecan-1. The data are the means ± S.E. *D*, extracts from tumors growing in animals injected with control or syn1A myeloma cells were resolved on SDS-PAGE and levels of human syndecan-1 (*Syn1*) assessed by Western blotting. The blot includes extracts of individual tumors from each of four animals from each group.

DISCUSSION

The findings presented here demonstrate that robust growth, angiogenesis, and metastasis of myeloma tumors *in vivo* are dependent on expression of adequate levels of syndecan-1. Utilizing myeloma cell lines having either syndecan-1 expression knocked out or knocked down, we made the following novel observations: (i) cells not expressing syndecan-1 became apoptotic *in vitro* and did not survive; (ii) cells in which syndecan-1 was knocked down to as low as 14% of wild-type syndecan-1 levels maintained their plasma cell phenotype and exhibited *in vitro* growth characteristics identical to those of control cells expressing wild-type levels of syndecan-1; (iii) in contrast to *in vitro* growth, growth of subcutaneously injected myeloma cells was highly dependent on the level of syndecan-1 expression with the decreased syndecan-1 expression correlating with poor tumor formation and growth; (iv) widespread

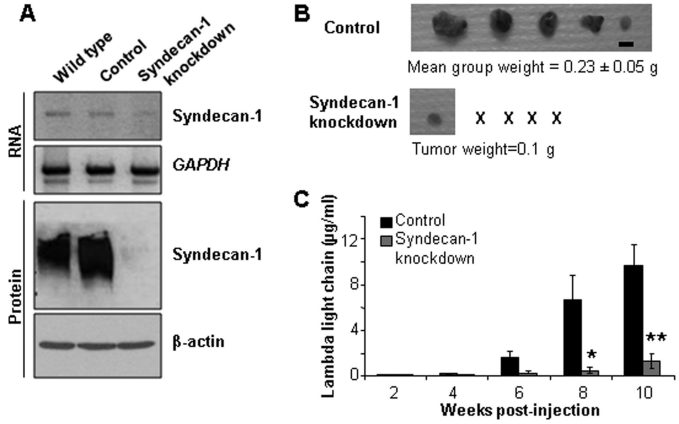

FIGURE 5. **Reduction of syndecan-1 levels in RPMI-8226 human myeloma cells yields results similar to CAG syndecan-1 knockdown cells.** *A*, knockdown of syndecan-1 upon transduction with the syn1A sequence was confirmed by RT-PCR (*upper two panels*) and Western blotting (*lower two panels*). The data are the means ± S.E. ($n = 3$). *B*, 5×10^6 control or knockdown cells were injected subcutaneously into the flanks of male SCID mice. At necropsy, the tumors were resected, weighed, and photographed (× represents animals with no detectable tumor; *bar*, 1 cm). *C*, murine sera were subjected to ELISA to assess levels of human immunoglobulin λ light chain as an indicator of whole animal tumor burden. The data are the means ± S.E. For control *versus* knockdown, *, $p = 0.042$; **, $p = 0.006$.

disseminated growth of myeloma, including growth within the bone marrow, was also dependent on the level of syndecan-1 expression; and (v) tumors formed by cells having diminished levels of syndecan-1 exhibited low levels of VEGF and impaired vascular development as compared with tumors expressing high levels of syndecan-1. It should be noted that both CAG and RPMI-8226 cell lines used in the present study grow rampantly *in vivo*, even outside of the bone marrow. The fact that knockdown of syndecan-1 expression can have such a dramatic effect on formation and growth of tumors derived from these aggressive cells points strongly to the importance of syndecan-1 in myeloma progression *in vivo*.

A critical role for syndecan-1 in regulating the growth of myeloma tumors has been implied by several previous studies, for example: (i) myeloma growth stimulated via signaling through HGF and epidermal growth factor family ligands is dependent on syndecan-1 heparan sulfate (27, 28); (ii) myeloma cells engineered to overexpress soluble syndecan-1 grow faster and metastasize better *in vivo* than do cells expressing wild-type levels of soluble syndecan-1 (14); (iii) the growth of freshly isolated tumor cells from myeloma patient bone marrow biopsies was inhibited in SCID-hu animals treated with heparinase III, an enzyme that destroys heparan sulfate (16); (iv) enhanced expression of Hsulf-1 or Hsulf-2, endosulfatases that specifically remove 6-*O* sulfate from heparan sulfate, inhibit myeloma tumor growth *in vivo* (29); (v) essentially all myeloma patient tumors isolated from the bone marrow are positive for syndecan-1 expression, and most of the cells within the tumors are positive for syndecan-1 (11); and (vi) similar to our findings, it has been reported that, in myeloma patients, the population of cells lacking syndecan-1 expression within a tumor are undergoing apoptosis (30). Thus, our present findings are consistent with these previous observations regarding syndecan-1 and heparan sulfate and, for the first time, definitively demonstrate the requirement for syndecan-1 for robust myeloma growth, angiogenesis, and dissemination. Given that previous studies have shown that heparan sulfate-degrading enzymes (heparinase III and HSulfs as mentioned above) inhibit myeloma growth *in vivo*; at least some, if not all, of the inhibitory effect of syndecan-1 knockdown is almost certainly due to the decrease in tumor heparan sulfate. In fact, loss of syndecan-1 expression removes almost all heparan sulfate from myeloma cells that express syndecan-1 as their predominant heparan sulfate proteoglycan (24). In addition, it is also possible that loss of the syndecan-1 core protein could affect tumor growth via decreased integrin activation (21).

A key finding of the present work is that cells low in syndecan-1 expression form metastatic lesions poorly following intravenous injection. In contrast, cells expressing wild-type levels of syndecan-1 exhibit extensive dissemination, including growth within bones. Although there is still a debate regarding whether myeloma metastases are seeded by tumor stem cells or by mature myeloma cells (or by both), there is ample evidence that mature plasma cells are involved. In the majority of myeloma patients, tumor cells readily intravasate into the blood and can be detected by flow cytometry (31). It has been demonstrated that these mature ($CD38^+/CD45^-$) syndecan-1-positive plasma cells isolated from the blood of myeloma patients can populate a nonmyelomatous human bone and produce disease that is typical of human myeloma (32, 33). Thus circulating, mature plasma cells in patients likely contribute to establishing new tumor foci leading to widely disseminated disease, a hallmark of myeloma (34). Although the mechanisms mediating metastasis of myeloma tumors are not well understood, they likely involve participation of a number of adhesion molecules, cytokines and proteases (34). Our results indicate that syndecan-1 plays a critical role in ensuring that tumor cells form metastatic foci following their intravasation into the circulation. A role for syndecan-1 in myeloma metastasis was also demonstrated in a previous study where we discovered that elevation of expression of shed syndecan-1 enhanced spontaneous metastasis from one bone to another bone (14).

At present, we do not know how syndecan-1 contributes to the post-intravasation metastatic events observed following intravenous injection of tumor cells. Given the broad array of interactions between syndecan-1 heparan sulfate and growth factors, cytokines, and adhesion molecules (5), syndecan-1 could be aiding enhanced survival of cells in the circulation, attachment of cells to secondary sites, and/or enhanced survival of the cells once they have homed to the secondary site. However, regardless of the mechanism of syndecan-1 function, our findings indicate that disabling syndecan-1 on circulating tumor cells of myeloma patients may block or diminish metastatic tumor growth.

It is intriguing that a reduction in syndecan-1 levels to as low as 14% of normal levels (syn1A cells) had little effect on myeloma growth *in vitro*, yet it dramatically impacted growth *in vivo*. This strongly suggests that diminished syndecan-1 expression does not have a direct effect on tumor cells but may substantially impact tumor-host interactions required for tumor survival and growth. This possibility is supported by our finding that VEGF levels within the tumors formed by syndecan-1 knockdown cells are low and that angiogenesis is impaired. Angiogenesis is a critical component of myeloma progression, and VEGF plays a determining role in inducing the angiogenic response (35, 36). It has been

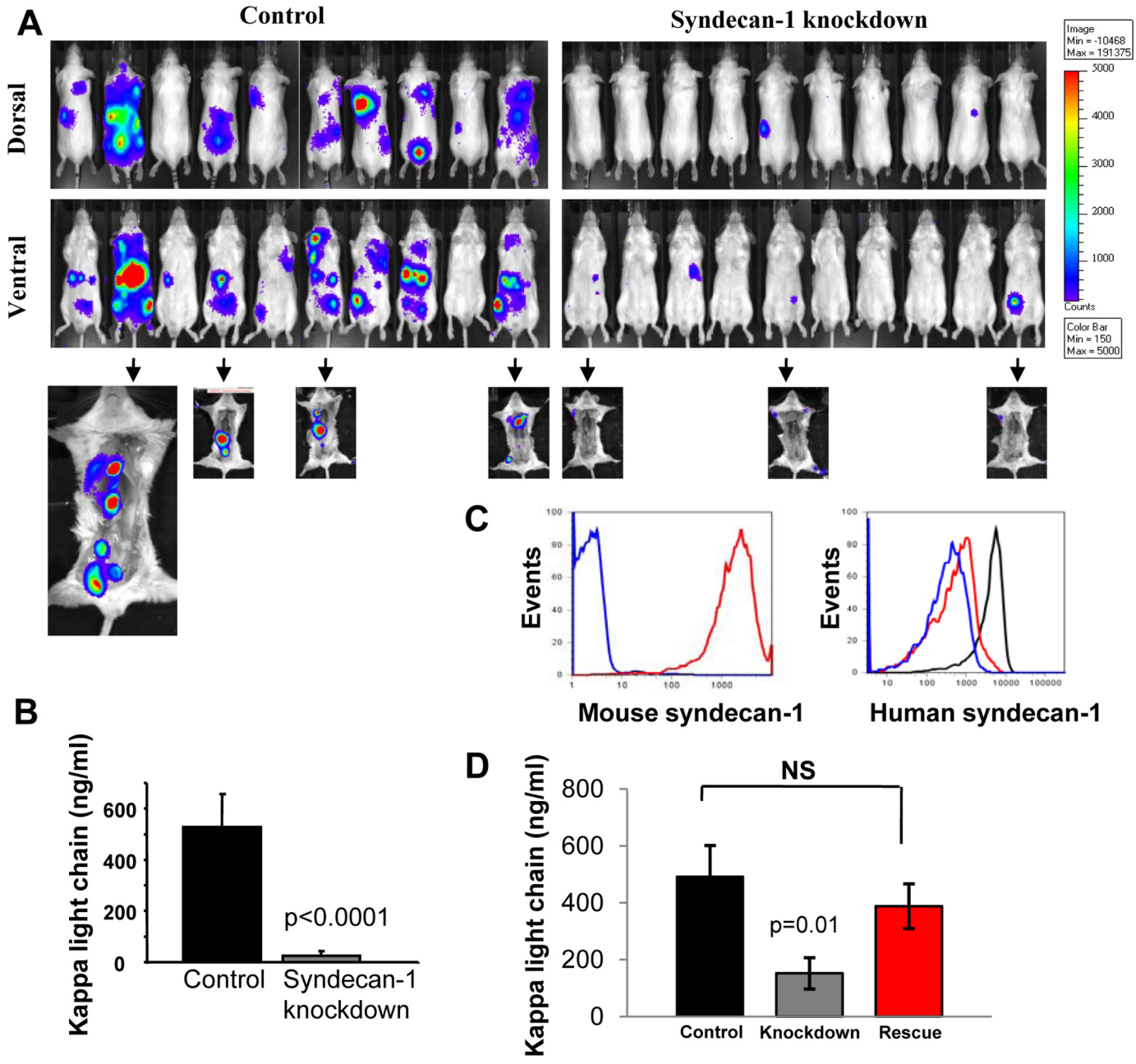

FIGURE 6. **Knockdown of syndecan-1 dramatically inhibits disseminated growth of myeloma.** Luciferase-tagged CAG control and syn1A knockdown cells were injected via tail vein into male SCID mice (experimental metastasis model). *A*, dorsal and ventral bioluminescent images shown are from all animals in a single experiment 5 weeks after the injection of tumor cells and are representative of two independent experiments (total animal number from two experiments: control, $n = 18$; syn1A, $n = 20$). *Arrows* point to images from animals following removal of visceral organs. Control cells showed a higher propensity toward growth in the bone as compared with knockdown cells. *B*, murine sera were collected at termination of the experiment and subjected to ELISA to assess levels of human immunoglobulin κ light chain as an indicator of whole animal tumor burden. The data are the means $\pm$ S.E. *C*, CAG syndecan-1 knockdown cells stably transfected to express full-length mouse syndecan-1 core protein were stained with 281.2 antibody (*red*) that specifically recognizes murine syndecan-1 or with control IgG (*blue*) and analyzed by flow cytometry. Expression of human syndecan-1 was also assessed in control (*black*) and syndecan-1 knockdown cells pre- (*blue*) and post-transfection (*red*) with mouse syndecan-1. The gates were set on live, GFP+ cells. *D*, 5×10^6 control, syndecan-1 knockdown, and knockdown cells expressing murine syndecan-1 (rescue cells) were injected intravenously into male SCID mice. Mouse serum was subjected to ELISA to assess levels of human immunoglobulin κ light chain as an indicator of whole animal tumor burden. The data are the means $\pm$ S.E. The data shown are from all of the animals (control, $n = 10$; syn1A, $n = 10$; mouse rescue, $n = 9$) in a single 5-week experiment and are representative of two independent studies. *NS*, not significant.

reported that myeloma cells overexpress and secrete VEGF, which acts to stimulate proliferation and chemotaxis of endothelial cells (37). Thus, following knockdown of syndecan-1, the impaired vessel formation that we observed may be due to the reduced levels of VEGF. However, other mechanisms may also be involved. For example, because some isoforms of VEGF bind to heparan sulfate, the diminished level of cell surface or shed syndecan-1 within the tumor could decrease the amount of VEGF retained within the tumor leading to the impaired angiogenic response. Also, it has been demonstrated that heparin can enhance VEGF-mediated receptor signaling and the resulting endothelial proliferation and tube formation (38) and that heparan sulfate *in trans* can potentiate the VEGF receptor signaling pathway leading to angiogenesis (39). Thus, it is possible that VEGF in a complex with syndecan-1

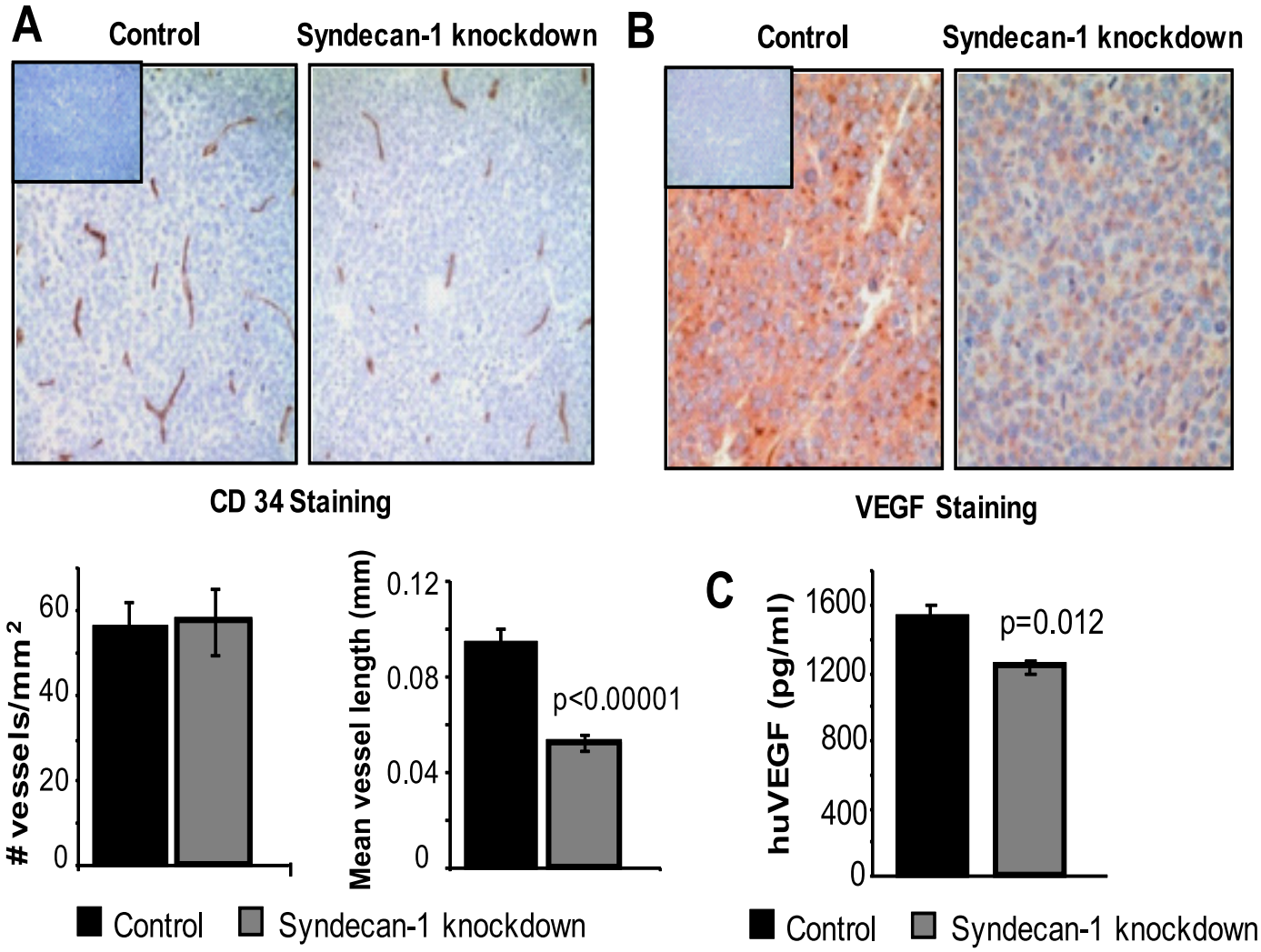

FIGURE 7. **Tumors formed by syndecan-1 knockdown cells have a poorly developed vasculature and decreased levels of human VEGF.** *A*, immunohistochemistry of xenograft tumor tissues from tumors formed by control or syn1A knockdown cells and stained with antibody to CD34 (*brown*) and counterstained with hematoxylin (*blue*) (original magnification, ×200). *Inset*, negative control. *Bar graphs*, quantification of microvessel density and average vessel length. The data are the means ± S.E. *B*, immunohistochemistry for human VEGF (*brown*) in xenograft tumor sections counterstained with hematoxylin (*blue*). *Inset*, antibody negative control (original magnification, ×400). *C*, medium conditioned by myeloma cells for 48 h was collected and levels of human VEGF assessed by ELISA. The data are the means ± S.E. ($n = 3$).

heparan sulfate provides enhanced VEGF receptor signaling, thereby promoting a robust angiogenic response.

Lastly, it has been proposed that syndecan-1-negative myeloma cells represent the myeloma stem cell compartment because they exhibit enhanced clonogenicity as compared with syndecan-1-positive cells (22, 40). In our studies, control cells with normal levels of syndecan-1 and knockdown cells expressing as low as 14% of the normal levels of syndecan-1 exhibited no difference in their colony forming potential. We did not test the population of cells that were syndecan-1-negative in colony forming assays but did observe that these cells became apoptotic and failed to survive in routine suspension culture. But regardless of the location and phenotype of the myeloma stem cells, the bulk of myeloma tumor cells in patients are mature, syndecan-1-positive plasma cells. These cells may gain the capacity for self-renewal as the myeloma tumor progresses, supported by the finding that patient bone marrow aspirates depleted of mature plasma cells could not establish tumors following their transplantation directly into human bones (SCID-hu model), whereas the mature (syndecan-1-positive) myeloma cells present in the blood or bone marrow successfully established tumors (32, 33). Thus, therapeutic targeting of the syndecan-1-positive population consisting of mature myeloma tumor cells may significantly diminish expansion of the tumor. Moreover, a reduction in syndecan-1 levels within the tumor would likely impinge upon multiple signaling pathways that are mediated by syndecan-1 heparan sulfate and, as our data demonstrate, could substantially inhibit widespread tumor growth and dissemination.

Acknowledgments—We thank Dr. Anne Woods (University of Alabama at Birmingham) for syndecan-2 and -4 antibodies, Dr. Danny Welch (University of Alabama at Birmingham) for assistance with the experimental metastasis model, Dr. Didier Trono (Ecole Polytechnique Fédérale de Lausanne) for providing lentiviral vectors, and Dr. Alan Rapraeger (University of Wisconsin, Madison) for polyclonal antibodies to syndecan-1.

REFERENCES

1. Barlogie, B., Shaughnessy, J., Epstein, J., Sanderson, R., Anaissie, E., Walker, R., and Tricot, G. (2006) in *Williams Hematology* (Lichtman, M. A., Beutler, E., Kipps, T. J., Seligsohn, U., Kaushansky, K., and Prchal, J. T. eds) 7th Ed., pp. 1501–1533, McGraw-Hill, New York
2. Anderson, K. C. (2007) *Exp. Hematol.* **35,** 155–162
3. Roodman, G. D. (2002) *J. Bone Miner. Res.* **17,** 1921–1925
4. Caers, J., Van Valckenborgh, E., Menu, E., Van Camp, B., and Vanderkerken, K. (2008) *Bull. Cancer* **95,** 301–313
5. Sanderson, R. D., and Yang, Y. (2008) *Clin. Exp. Metastasis* **25,** 149–159
6. Perez, L. E., Parquet, N., Shain, K., Nimmanapalli, R., Alsina, M., Anasetti, C., and Dalton, W. (2008) *J. Immunol.* **180,** 1545–1555
7. Alexander, C. M., Reichsman, F., Hinkes, M. T., Lincecum, J., Becker, K. A., Cumberledge, S., and Bernfield, M. (2000) *Nat. Genet.* **25,** 329–332
8. Maeda, T., Alexander, C. M., and Friedl, A. (2004) *Cancer Res.* **64,** 612–621
9. Aikawa, T., Whipple, C. A., Lopez, M. E., Gunn, J., Young, A., Lander, A. D., and Korc, M. (2008) *J. Clin. Invest.* **118,** 89–99
10. Wijdenes, J., Vooijs, W. C., Clément, C., Post, J., Morard, F., Vita, N., Laurent, P., Sun, R. X., Klein, B., and Dore, J. M. (1996) *Br. J. Haematol.* **94,** 318–323
11. Bayer-Garner, I. B., Sanderson, R. D., Dhodapkar, M. V., Owens, R. B., and Wilson, C. S. (2001) *Mod. Pathol.* **14,** 1052–1058
12. Seidel, C., Børset, M., Hjertner, O., Cao, D., Abildgaard, N., Hjorth-Hansen, H., Sanderson, R. D., Waage, A., and Sundan, A. (2000) *Blood* **96,** 3139–3146
13. Bartlett, A. H., Hayashida, K., and Park, P. W. (2007) *Mol. Cells* **24,** 153–166
14. Yang, Y., Yaccoby, S., Liu, W., Langford, J. K., Pumphrey, C. Y., Theus, A., Epstein, J., and Sanderson, R. D. (2002) *Blood* **100,** 610–617
15. Anderson, K. C., and Dalton, W. S. (2002) *Mol. Cancer Ther.* **1,** 1361–1365
16. Yang, Y., MacLeod, V., Dai, Y., Khotskaya-Sample, Y., Shriver, Z., Venkataraman, G., Sasisekharan, R., Naggi, A., Torri, G., Casu, B., Vlodavsky, I., Suva, L. J., Epstein, J., Yaccoby, S., Shaughnessy, J. D., Jr., Barlogie, B., and Sanderson, R. D. (2007) *Blood* **110,** 2041–2048
17. Børset, M., Hjertner, O., Yaccoby, S., Epstein, J., and Sanderson, R. D. (2000) *Blood* **96,** 2528–2536
18. Saunders, S., Jalkanen, M., O'Farrell, S., and Bernfield, M. (1989) *J. Cell Biol.* **108,** 1547–1556
19. Jalkanen, M., Nguyen, H., Rapraeger, A., Kurn, N., and Bernfield, M. (1985) *J. Cell Biol.* **101,** 976–984
20. Purushothaman, A., Chen, L., Yang, Y., and Sanderson, R. D. (2008) *J. Biol. Chem.* **283,** 32628–32636
21. Beauvais, D. M., Burbach, B. J., and Rapraeger, A. C. (2004) *J. Cell Biol.* **167,** 171–181
22. Matsui, W., Huff, C. A., Wang, Q., Malehorn, M. T., Barber, J., Tanhehco, Y., Smith, B. D., Civin, C. I., and Jones, R. J. (2004) *Blood* **103,** 2332–2336
23. Dalton, W., and Anderson, K. C. (2006) *Clin. Cancer Res.* **12,** 6603–6610
24. Yang, Y., Macleod, V., Miao, H. Q., Theus, A., Zhan, F., Shaughnessy, J. D., Jr., Sawyer, J., Li, J. P., Zcharia, E., Vlodavsky, I., and Sanderson, R. D. (2007) *J. Biol. Chem.* **282,** 13326–13333
25. Derksen, P. W., Keehnen, R. M., Evers, L. M., van Oers, M. H., Spaargaren, M., and Pals, S. T. (2002) *Blood* **99,** 1405–1410
26. Dvorak, H. F., Brown, L. F., Detmar, M., and Dvorak, A. M. (1995) *Am. J. Pathol.* **146,** 1029–1039
27. Derksen, P. W., Keehnen, R. M., Evers, L. M., van Oers, M. H., Spaargaren, M., and Pals, S. T. (2002) *Blood* **99,** 1405–1410
28. Mahtouk, K., Cremer, F. W., Rème, T., Jourdan, M., Baudard, M., Moreaux, J., Requirand, G., Fiol, G., De Vos, J., Moos, M., Quittet, P., Goldschmidt, H., Rossi, J. F., Hose, D., and Klein, B. (2006) *Oncogene* **25,** 7180–7191
29. Dai, Y., Yang, Y., MacLeod, V., Yue, X., Rapraeger, A. C., Shriver, Z., Venkataraman, G., Sasisekharan, R., and Sanderson, R. D. (2005) *J. Biol. Chem.* **280,** 40066–40073
30. Jourdan, M., Ferlin, M., Legouffe, E., Horvathova, M., Liautard, J., Rossi, J. F., Wijdenes, J., Brochier, J., and Klein, B. (1998) *Br. J. Haematol.* **100,** 637–646
31. Witzig, T. E., Kimlinger, T. K., Ahmann, G. J., Katzmann, J. A., and Greipp, P. R. (1996) *Cytometry* **26,** 113–120
32. Yaccoby, S., Barlogie, B., and Epstein, J. (1998) *Blood* **92,** 2908–2913
33. Yaccoby, S., and Epstein, J. (1999) *Blood* **94,** 3576–3582
34. Vande Broek, I., Vanderkerken, K., Van Camp, B., and Van Riet, I. (2008) *Clin. Exp. Metastasis* **25,** 325–334
35. Ribatti, D., Nico, B., and Vacca, A. (2006) *Oncogene* **25,** 4257–4266
36. Ribatti, D., and Vacca, A. (2008) *Genes Nutr.* **3,** 29–34
37. Vacca, A., Ria, R., Ribatti, D., Semeraro, F., Djonov, V., Di Raimondo, F., and Dammacco, F. (2003) *Haematologica* **88,** 176–185
38. Ashikari-Hada, S., Habuchi, H., Kariya, Y., and Kimata, K. (2005) *J. Biol. Chem.* **280,** 31508–31515
39. Jakobsson, L., Kreuger, J., Holmborn, K., Lundin, L., Eriksson, I., Kjellén, L., and Claesson-Welsh, L. (2006) *Dev. Cell* **10,** 625–634
40. Kukreja, A., Hutchinson, A., Dhodapkar, K., Mazumder, A., Vesole, D., Angitapalli, R., Jagannath, S., and Dhodapkar, M. V. (2006) *J. Exp. Med.* **203,** 1859–1865